Theoretical Study of the Interaction of Water and Imidazole with Iron and Nickel Dications

Alessandra Ricca* and Charles W. Bauschlicher, Jr.†

NASA Ames Research Center, Moffett Field, California 94035

Received: November 9, 2001

The structures, the harmonic frequencies, and the energies of $Fe(H_2O)_n(imid)_m^{2+}$ and $Ni(H_2O)_n(imid)_m^{2+}$ complexes are computed using density functional theory with the B3LYP functional. A CSOV analysis shows that the bonding is mostly electrostatic in nature. Imidazole forms a stronger bond than water with both metal dications because of its larger dipole moment and polarizability. The reactions for the exchange of one water molecule by one imidazole are exothermic, and up to six water molecules can be replaced by imidazoles. The trends are very similar for both metals with the displacement reactions being slightly more favorable for Ni^{2+}.

I. Introduction

Currently there is considerable interest in obtaining metallic protein nanotubes. Protein nanotubes can be obtained by self-assembly and can be genetically engineered to obtain other nanostructures. Building blocks of these nanostructures are double-ring structures named chaperonins which can survive extreme conditions such as a pH of 3.0 and a temperature of 83 °C and which associate to form tubes and filaments.[1] The chaperonins consist of 60 kDa heat shock protein (HSP60) subunits.[1−4] The structure of the subunits can be manipulated genetically to influence their assembly, strength, and binding properties. Amino acid "tails" consisting of one histidine residue bound to an aliphatic chain have been attached to HSP60s with the aim of binding metals, such as iron and nickel, inside the HSP60 structure.[5] These histidine tails have been designed to have flexibility and should be less restricted in their motion than the histidine residues in the double rings. To form a complex with a positively charged metal in water, the histidine has to displace the waters around the metal ion. Several theoretical studies have been performed on the binding of Zn^{2+}, Mg^{2+}, and Ca^{2+} with imidazoles and waters.[6−11] All of these studies show that imidazole can displace water attached to the metal ion which is consistent with the fact that metalloenzymes are stable in an aqueous environment. However, the Zn^{2+}, Mg^{2+}, and Ca^{2+} ions are closed shell systems, and there is a lack of information on dications with open shell d orbitals such as Fe^{2+} and Ni^{2+}.

The scope of this study is to study the successive exchange of one water molecule by one imidazole for both Fe^{2+} and Ni^{2+} and to understand how the presence of d electrons influences the exchange energies. As a first step, we perform our calculations in the gas phase. We use the hexacoordinated $M(H_2O)_6^{+2}$ ions as models of the hydration because a coordination of 6 is known to be prevalent,[12,13] and we use the imidazole molecule as a model of the histidine residue. Further calculations including the effect of solvation and of the protein will be required in the design of protein nanotubes.

* To whom correspondence should be addressed. E-mail: ricca@pegasus.arc.nasa.gov. ELORET Corp., Mail Stop 230-3.

† Space Technology Division, Mail Stop 230-3.

II. Methods

The geometries are optimized using density functional theory (DFT), in conjunction with the hybrid[14] B3LYP[15] approach. We use the 6-31+G basis set to describe the transition metal atom and the 6-31G basis set for the other atoms.[16−19] This basis set is denoted as "small". The harmonic vibrational frequencies are computed at the same level of theory as the geometry optimization, and the zero-point energy is computed as one-half the sum of the B3LYP harmonic frequencies, which are not scaled.

Calibration calculations are performed for the dissociation of $Ni(H_2O)_6^{2+}$ to Ni^{2+} and six H_2O molecules using the Hartree−Fock (HF) and B3LYP approaches in conjunction with the 6-31G, 6-311G**, 6-311++G**, and 6-311++G(2df,2p) basis sets.[16−19] On the basis of these calibration calculations, the B3LYP/6-311++G** reaction energies for the exchange of one water molecule by an imidazole molecule, such as

$$M^{2+}(H_2O)_n(Imid)_m + Imid \rightarrow M^{2+}(H_2O)_{n-1}(Imid)_{m+1} + H_2O \quad (1)$$

are calculated at the B3LYP/small optimized geometries. The B3LYP/small zero-point energies are added to the reaction energies. All of the DFT calculations are performed using Gaussian 98.[20]

The bonding is analyzed using the constrained space orbital variation (CSOV) technique,[21] where the Hartree−Fock (HF) wave function is optimized in a series of steps that allow a decomposition of the bonding. The specific steps are discussed in more detail below. The CSOV calculations are performed at the B3LYP/small geometry. The metal basis sets are the Wachter/Hay[17,18] sets with a (3f)/[1f] polarization function.[22] The ligand valence basis sets are taken from the correlation consistent polarized valence triple-ζ (cc-pVTZ) sets.[23] A single polarization function is added to each basis set, and they are taken from the cc-pV double-ζ sets. The CSOV calculations are performed using MOLECULE-SWEDEN.[24]

III. Results and Discussion

This section is divided into three subsections. In the first subsection, we describe the geometries and electron occupations of the complexes studied. In the second subsection, we describe

10.1021/jp014133y CCC: $22.00
Published on Web 03/08/2002

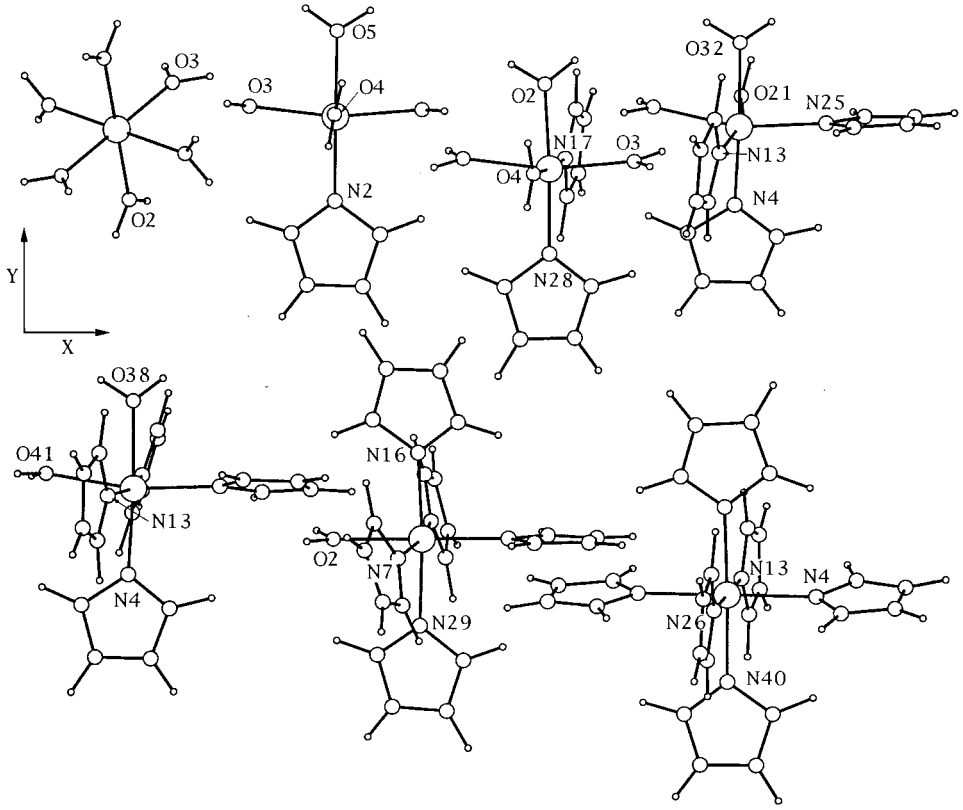

Figure 1. B3LYP/small optimized geometries for $Fe(H_2O)_{6-m}imid_m^{2+}$, for $m = 0-6$. The atom labels are the same as those used in Table 1. The *x* and *y* axes are shown on the figure, and the *z* axis is perpendicular to the page.

TABLE 1: Geometries of $Fe(H_2O)_n(imid)_{6-n}^{2+}$ ($n = 0-6$), and $Ni(H_2O)_n(imid)_{6-n}^{2+}$ ($n = 0-6$)

	distances			angles		
	parameter	Fe	Ni	parameter	Fe	Ni
$M(H_2O)_6^{2+}$	M−O	2.140	2.072	O2−M−O3	93.0	90.0
$M(H_2O)_5imid^{2+}$	M−N2	2.118	2.047	N2−M−O3	96.7	94.3
	M−O5	2.153	2.091	O3−M−O4	89.1	90.0
	M−O4	2.186	2.084	O4−M−O5	88.5	89.0
$M(H_2O)_4(imid)_2^{2+}$	M−O2	2.172	2.143	O3−M−O2	85.3	88.2
	M−O4	2.206	2.098	O4−M−N17	176.1	175.1
	M−N28	2.133	2.065	N17−M−N28	96.2	96.4
$M(H_2O)_3(imid)_3^{2+}$	M−N4	2.152	2.086	N4−M−N13	95.3	95.8
	M−O21	2.257	2.140	O21−M−N25	93.3	94.5
	M−O32	2.167	2.137	O21−M−O32	81.9	82.4
$M(H_2O)_2(imid)_4^{2+}$	M−N4	2.173	2.102	N4−M−N13	90.7	91.5
	M−N13	2.203	2.132	N4−M−O38	176.4	176.0
	M−O38	2.210	2.173	N4−M−O41	95.2	95.5
$MH_2O(imid)_5^{2+}$	M−O2	2.228	2.189	O2−M−N7	84.6	85.2
	M−N7	2.231	2.142	O2−M−N16	89.6	89.6
	M−N29	2.221	2.144	N7−M−N16	90.5	89.6
$M(imid)_6^{2+}$	M−N4	2.254	2.167	N4−M−N13	90.2	90.3
	M−N40	2.236	2.166	N26−M−N40	91.4	89.7

our calibration calculations for the computation of the ligand exchange energetics. These include a basis set study and a CSOV analysis of the bonding. The third subsection contains our best estimates for the ligand exchange reaction energies.

A. Structures and Bonding. The structures of the Fe-containing species are shown in Figure 1. The structures of the Ni-containing systems are very similar to those for the Fe-containing species and are therefore not given. The metal−ligand bond lengths and selected ligand−metal−ligand angles are given in Table 1. From Table 1 we observe that the Ni−L distances are slightly shorter than the analogous Fe−L distances, but the angles for analogous Fe and Ni-containing systems are very similar. The metal d populations and the metal spins (spin denotes 2S) are given in Table 2. Table 2 shows that for all of the iron-containing systems the bonding is derived from a d^6 metal occupation, and the Fe spin is around 3.8, whereas for nickel-containing systems the bonding is derived from a d^8 metal occupation, and the Ni spin is between 1.6 and 1.8.

TABLE 2: Metal d_σ, d_{xz}, d_{yz}, $d_{x^2-y^2}$, and d_{xy} Spins, Total Metal Spin, and Metal d Population, Computed Using a Mulliken Population Analysis of the B3LYP/Small Wave Functions

	d_σ	d_{xz}	d_{yz}	$d_{x^2-y^2}$	d_{xy}	$spin_{tot}$	d_{pop}
$Fe(H_2O)_6^{2+}$ ^5A (C_3)	0.00	0.95	0.95	0.95	0.95	3.84	6.26
$Ni(H_2O)_6^{2+}$ ^3A_g (T_h)	0.90	0.00	0.00	0.90	0.00	1.80	8.21
$Fe(H_2O)_5imid^{2+}$ $^5A''$ (C_s)	0.93	0.21	0.76	0.91	0.98	3.84	6.24
$Ni(H_2O)_5imid^{2+}$ $^3A'$ (C_s)	0.90	0.00	0.00	0.87	0.00	1.77	8.22
$Fe(H_2O)_4(imid)_2^{2+}$ ^5A (C_1)	0.93	0.05	0.93	0.97	0.89	3.83	6.22
$Ni(H_2O)_4(imid)_2^{2+}$ ^3A (C_1)	0.89	0.00	0.00	0.02	0.83	1.74	8.22
$Fe(H_2O)_3(imid)_3^{2+}$ ^5A (C_1)	0.97	0.88	0.62	0.64	0.65	3.82	6.21
$Ni(H_2O)_3(imid)_3^{2+}$ ^3A (C_1)	0.00	0.57	0.57	0.29	0.29	1.72	8.22
$Fe(H_2O)_2(imid)_4^{2+}$ ^5A (C_1)	0.56	0.78	0.91	0.78	0.73	3.82	6.19
$Ni(H_2O)_2(imid)_4^{2+}$ ^3A (C_1)	0.24	0.00	0.82	0.63	0.00	1.69	8.21
$FeH_2O(imid)_5^{2+}$ ^5A (C_1)	0.90	0.92	0.32	0.86	0.75	3.81	6.17
$NiH_2O(imid)_5^{2+}$ ^3A (C_1)	0.85	0.00	0.00	0.81	0.01	1.67	8.21
$Fe(imid)_6^{2+}$ ^5A_g (C_i)	0.95	0.92	0.29	0.97	0.62	3.80	6.15
$Ni(imid)_6^{2+}$ ^3A_g (C_i)	0.41	0.44	0.12	0.14	0.54	1.65	8.20

$Ni(H_2O)_6^{2+}$ has an octahedral geometry (T_h) and a ^3A_g ground state. This geometrical arrangement has the optimal ligand-field stabilization and is predicted to be very stable. The two e_g orbitals (d_σ and $d_{x^2-y^2}$) which both point toward the in-plane lone pairs of the oxygens are singly occupied to reduce the repulsion.

$Fe(H_2O)_6^{2+}$ has C_3 symmetry and a ^5A ground state. The only doubly occupied d orbital is aligned along the C_3 axis, which points between the ligands, to reduce the repulsion with the ligands. Although the C_3 configuration has a larger ligand−ligand repulsion than the T_h one, it reduces the metal−ligand repulsion for the iron with four open shell d orbitals by more than it increases the ligand−ligand repulsion.

Replacing one water by a imidazole in $Ni(H_2O)_6^{2+}$ leads to a molecule with C_s symmetry and a $^3A'$ ground state. As for $Ni(H_2O)_6^{2+}$, the d_σ and the $d_{x^2-y^2}$ orbitals, which point toward the in-plane lone pairs of the oxygens, contain the two unpaired electrons to minimize the metal−ligand repulsion. The presence of the imidazole ligand hardly affects the geometry of the $Ni(H_2O)_5$ part of the complex.

$Fe(H_2O)_5(imid)^{2+}$ has C_s symmetry and a $^5A''$ ground state. The doubly occupied orbital is a d_π orbital consisting mostly of d_{xz} with some d_{yz} mixed in. The mixing results in the doubly occupied orbital bissecting an O−Fe−O angle to minimize the repulsion with the ligands.

$Ni(H_2O)_4(imid)_2^{2+}$ has C_1 symmetry and a ^3A ground state. The structure is derived from $Ni(H_2O)_5imid^{2+}$ by replacing a water molecule in an equatorial position by an imidazole and has a configuration with water molecules opposite to the imidazole ligands. By placing a water molecule opposite to an imidazole, the d orbitals on the metal can polarize away from the nitrogen toward the oxygens and reduce the metal−ligand repulsion. This effect is larger than the ligand−ligand repulsion which favors two imidazole ligands in axial positions.

$Fe(H_2O)_4(imid)_2^{2+}$, like $Ni(H_2O)_4(imid)_2^{2+}$, is derived from $Fe(H_2O)_5imid^{2+}$ by replacing a water molecule in an equatorial position by an imidazole. The molecule has C_1 symmetry and a ^5A ground state. The doubly occupied orbital is mainly a d_{xz} orbital with some mixing of the d_{yz} orbital. The mixing allows the doubly occupied orbital to tilt away from the *xz* plane and reduce the repulsion with the ligands.

As for $Ni(H_2O)_4(imid)_2^{2+}$, the structure lowest in energy for $Ni(H_2O)_3(imid)_3^{2+}$ has the three imidazole ligands opposite to the waters. $Ni(H_2O)_3(imid)_3^{2+}$ has C_1 symmetry and a ^3A ground state. The repulsion between the three bulky imidazoles affects the structure which differs now considerably from the octahedral geometry of $Ni(H_2O)_6^{2+}$. The waters move close toward each other, and the ligands do not point directly toward each other. The two singly occupied orbitals reduce the metal−ligand repulsion by pointing toward the ligands. The d orbitals are mixed in character as shown in Table 2.

$Fe(H_2O)_3(imid)_3^{2+}$ has a ^5A ground state with C_1 symmetry. The structure of the ground state is similar to the one for $Ni(H_2O)_3(imid)_3^{2+}$. The Fe doubly occupied orbital is located in a plane bissecting one water and one imidazole, and three singly occupied orbitals point toward the lone pairs of the ligands. As for $Ni(H_2O)_3(imid)_3^{2+}$, the d orbitals are mixed in character.

$Ni(H_2O)_2(imid)_4^{2+}$ has a structure containing two imidazole ligands opposite to each other. To reduce the repulsion between the imidazole ligands, the N−Ni−N angles are now close to 90°. The structure of $Ni(H_2O)_2(imid)_4^{2+}$ is more similar to that of $Ni(H_2O)_4(imid)_2^{2+}$ than that of $Ni(H_2O)_3(imid)_3^{2+}$. This is also apparent from the orbitals which show less mixing. $Ni(H_2O)_2(imid)_4^{2+}$ has a ^3A ground state with C_1 symmetry. The lone pairs of the two nitrogens in the *xz* plane are bulkier than those of the oxygens and the d orbital polarizes away from the nitrogens toward the oxygens. $Fe(H_2O)_2(imid)_4^{2+}$ has a ^5A ground state with C_1 symmetry and a structure similar to the one for $Ni(H_2O)_2(imid)_4^{2+}$.

$Ni(H_2O)(imid)_5^{2+}$ has a ^3A ground state with C_1 symmetry. Replacing one water with one imidazole increases the angle between the remaining water and the new imidazole to a value of 89.6 versus 80.7 for the two waters of $Ni(H_2O)_2(imid)_4^{2+}$. Overall the angles between the ligands are close to 90°, and the orbitals show less mixing. $Fe(H_2O)(imid)_5^{2+}$ has a ^5A ground state with C_1 symmetry a structure similar to the one of $Ni(H_2O)(imid)_5^{2+}$.

TABLE 3: Dissociation Energies (in kcal/mol) for $Ni(H_2O)_6^{2+}$ Leading to Ni^{2+} and Six H_2O Molecules Computed at the Hartree−Fock and B3LYP Levels of Theory for Various Basis Sets

	6-31G	small	6-311G**	6-311++G**	6-311++G(2df,2p)
D_e HF	392.7	392.1	344.4	327.3	321.7
D_e B3LYP	438.6	440.4	392.3	362.8	356.4
Δ	45.9	48.3	47.9	35.5	34.7

$Ni(imid)_6^{2+}$ has a ^3A_g ground state with C_i symmetry. This configuration with centrosymmetrical pairs of of imidazole rings has also been observed in the crystal structure of hexakis(imidazole)nickel(II)nitrate.[25] The X-ray structure consists of a nickel atom at the center of a slightly compressed octahedron of nitrogen atoms. The six imidazoles are crystallographically identical, and the binding takes place though the pyridine type nitrogen instead of the pyrrole (N−H) nitrogen. In each pair of imidazoles, the N−H bonds are anti to each other, and this orientation maximizes the ligand−ligand dipole−dipole interaction. In our computed geometry, the imidazoles deviate by only 7° from the plane defined by one nitrogen of one pair, the Ni atom, and the nitrogen of the other pair. The doubly occupied orbitals avoid the repulsion with the ligands by pointing between them. $Fe(imid)_6^{2+}$ has a ^5A_g ground state with C_i symmetry.

B. Calibration Calculations. The basis set calibration calculations are given in Table 3, where we consider both the HF and B3LYP binding energies. $Ni(H_2O)_6^{2+}$ is used because the high symmetry makes the calculations quite tractable even in the largest basis set. The values in the 6-31G and "small" sets are very similar, thus, improving the metal basis set has resulted in only a small change in the binding energy. Improving the valence basis set and adding polarization functions results in a sizable reduction in the binding energies. This suggests that improving the basis set has reduced the basis set superposition error (BSSE). Adding diffuse functions, i.e., the difference between 6-311G** and 6-311++G** basis sets, results in another reduction in the binding energy and the difference between the HF and B3LYP results is smaller. A further extension of the polarization functions makes a small change in the binding energy. On the basis of these calibration calculations, it is clear that accurate ligand reaction energies will require a basis set larger than the "small" set, used to optimize the geometries, and we choose the 6-311++G** set as a compromise between accuracy and affordability. However, it is clear that further basis set expansions will reduce our total ligand binding energies slightly, but because the small total error is spread over six ligands and there should be some cancellation of errors, we feel that the B3LYP ligand exchange energetics will be accurate to about 2 kcal/mol.

The small difference between the B3LYP and HF binding energies suggests that the bonding in $Ni(H_2O)_6^{2+}$ is mostly electrostatic in nature. In Table 4, we report the results of CSOV calculations on $Fe(H_2O)_6^{2+}$, $Fe(H_2O)_5imid^{2+}$, $Ni(H_2O)_6^{2+}$, and $Ni(H_2O)_5imid^{2+}$ to see if this is a general feature of all of the systems studied in this work. We first note that the BSSE for the metal atoms is very small. The values for the ligands are somewhat larger but still a small fraction of the total binding energy. The ligand−ligand repulsion, computed as the energy difference between the ligands at infinite separation and at the geometry of the complex, are relatively similar for the four complexes studied. The values are slightly larger for the Ni systems because Ni^{2+} is smaller than Fe^{2+}, and hence, the ligands are closer together.

The first step in the CSOV is the frozen orbital energy where the energy of the complex is evaluated using the metal and

TABLE 4: CSOV Analysis of the Bonding[a]

	$Fe(H_2O)_6^{2+}$		$Fe(H_2O)_5imid^{2+}$	
Fe BSSE	0.2		0.2	
ligand BSSE	8.0		6.9	
ligand−ligand repulsion	37.6		38.4	
CSOV step	E	Δ	E	Δ
frozen orbital	−190.3		−189.1	
relax ligands	−285.2	−94.9	−306.1	−116.9
relax Fe	−285.9	−0.7	−307.2	−1.0
ligand donate	−305.9	−20.7	−314.5	−19.8
Fe donate	−309.4	−3.6	−331.2	−4.2
fully relaxed	−309.7	−0.3	−331.6	−0.5
	$Ni(H_2O)_6^{2+}$		$Ni(H_2O)_5imid^{2+}$	
Ni BSSE	0.3		0.3	
ligand BSSE	8.6		7.5	
ligand−ligand repulsion	41.8		43.3	
CSOV step	E	Δ	E	Δ
frozen orbital	−199.2		−196.9	
relax ligands	−306.2	−107.0	−327.6	−130.7
relax Ni	−307.2	−1.0	−328.8	−1.2
ligand donate	−330.3	−24.1	−338.5	−22.8
Ni donate	−334.4	−4.2	−356.7	−5.1
fully relaxed	−334.8	−0.4	−357.1	−0.5

[a] All energies are in kcal/mol.

ligand orbitals. In this step, the ligand occupied orbitals are Schmidt orthogonalized to the metal doubly occupied orbitals and the metal open-shell orbitals are Schmidt orthogonalized to the ligand occupied orbitals. Because the M^{2+} species do not have an occupied 4s orbital, there is very little metal−ligand repulsion, and all four systems are significantly bound at this step because of the electrostatic, charge−dipole, interaction. The shorter Ni-ligand bond length leads to a larger electrostatic stabilization than for the analogous Fe complex.

The second step is to allow the ligand occupied and virtual orbitals to mix; this step measures the ligand polarization without allowing any donation to the metal orbitals. The energy associated with this step is quite large. It is larger for $M(H_2O)_5imid^{2+}$ than for $M(H_2O)_6^{2+}$ because imidazole is more polarizable than water. The values are larger for Ni than Fe because of the shorter metal−ligand bond length. We should note that a comparison of the ligand properties at the HF and B3LYP levels, computed using the 6-311++G** basis set, shows that the water and imidazole dipole moments along the ligand−metal bond axis are decreased by 3.5 and 2.2%, respectively, but that the polarizablities are increased by 12.7 and 6.3% when the HF is replaced by the B3LYP. Thus, at the B3LYP level of theory, the frozen orbital value would be slightly smaller and the relaxation energy slightly larger, with the sum of the two terms being slightly larger than found at the HF level.

The third step relaxes the metal, and very little energy is gained. The fourth step allows the ligands to donate charge to the metal. This is actually done in two substeps to avoid the metal open-shell d orbitals mixing with virtual orbitals, because this could introduce metal donation into the ligand donation step. In the first substep, the metal occupied orbitals are frozen and the ligand is optimized with all virtuals. This allows the ligands to donate to the metal and also relax as they donate. In the second substep, the metal open-shells are allowed to mix with ligand occupied orbitals. The energy associated with ligand donation is small compared with the total binding energy. Because this step also introduces BSSE into the wave function, the true value is even smaller than that given in Table 4.

In the fifth CSOV step, the metal is allowed to donate to the ligands, and this is small, as expected. The final step is an unconstrained HF calculation, and the energy lowering associated with this step is very small; thus, we have no unaccounted for binding effects. The $Ni(H_2O)_6^{2+}$ total binding energy falls between the 6-311G** and 6-311++G** results showing that the CSOV basis set is capable of demonstrating the most important bonding effects.

TABLE 5: Reaction Energies (in kcal/mol) for the Exchange of One Water Molecule by One Imidazole Molecule[a]

	B3LYP/small		B3LYP/6-311++G**	
reactants	Fe	Ni	Fe	Ni
$M(H_2O)_6^{2+}$	−19.6	−22.1	−25.8	−27.7
$M(H_2O)_5imid^{2+}$	−16.9	−18.8	−22.0	−23.9
$M(H_2O)_4(imid)_2^{2+}$	−14.6	−16.3	−18.0	−21.3
$M(H_2O)_3(imid)_3^{2+}$	−11.3	−12.2	−16.5	−16.8
$M(H_2O)_2(imid)_4^{2+}$	−9.4	−10.2	−13.6	−14.9
$MH_2O(imid)_5^{2+}$	−7.5	−8.3	−13.7	−12.9

[a] The zero-point energy is included.

The CSOV analysis shows that the bonding is mostly electrostatic; ligand donation to the metal is less than 10% of the total HF binding energy. As noted above, the B3LYP is expected to slightly (less than 10 kcal/mol) increase the electrostatic bonding; thus, about 20 kcal/mol of the difference between the HF and B3LYP probably arises from an increase in the ligand to metal donation, which is underestimated at the HF level. However, even with this potential increase in the dative bonding, it is clear that the bonding in these systems is mostly electrostatic. This is consistent with the observation that the $Ni(H_2O)_6^{2+}$ binding energy decreases with basis set improvement. Because electrostatic bonding tends to be easier to describe than dative or covalent bonding, we believe that B3LYP ligand reaction energies in the 6-311++G** basis set should be accurate.

C. Reaction Energies. The reaction energies for the exchange of one water molecule by one imidazole are given in Table 5. The energies for the exchange of ligands are similar for the small and the 6-311++G** basis set, whereas the total dissociation energies (see Table 3) are very dependent on the basis sets. This supports the idea that some cancellation of errors occurs for the exchange of ligands and indicates that the values reported in Table 5 should be accurate. All of the reactions are exothermic, indicating that the bonding of Fe^{2+} and Ni^{2+} with imidazole is stronger than the one with water and that up to six waters can be replaced by imidazoles. As our CSOV analysis shows, the bonding is mostly electrostatic in nature. The experimental dipole moment of water is 1.85 D,[26] whereas the one for imidazole is 3.67 D.[27] Moreover, our computed average polarizability for water at the B3LYP/6-311++G** level of theory is 9.9 a_0^3 versus 46.6 a_0^3 for imidazole. Clearly, the bonding of imidazole with Fe^{2+} and Ni^{2+} is stronger than the one with water because of larger charge−dipole and charge−induced-dipole interactions. These results are consistent with previous experimental and theoretical results[7,10,11] which show that imidazole forms a very strong bond with doubly charged ions, such as Zn^{2+} and Mg^{2+}, and that imidazole can displace water. The reaction energies are similar for both metals with values slightly larger for Ni^{2+} because Ni^{2+} is smaller than Fe^{2+} and the electrostatic interactions are stronger. The trends are also similar for both metal ions. Replacing the first water by an imidazole is the most favorable reaction. Adding more imidazoles introduces more ligand−ligand repulsion and the reactions become less favorable by approximately 2 kcal/mol for each replacement. This reduction is relatively small considering the fact that the imidazole ligands are much bulkier than the waters. This is consistent with our CSOV analysis showing that the bonding is mainly electrostatic in nature with similar ligand−ligand repulsion. Note that the smaller size of

Ni^{2+} leads to an increased ligand−ligand repulsion, and for the sixth ligand replacement, the value for Ni is actually smaller than for Fe.

IV. Conclusions

The bonding for the $Fe(H_2O)_n(imid)_m^{2+}$ and $Ni(H_2O)_n(imid)_m^{2+}$ complexes is mainly due to electrostatic interactions. Imidazole forms a stronger bond than water with both Fe^{2+} and Ni^{2+} because of its larger dipole moment and polarizability. The reactions for the exchange of one water ligand by one imidazole are exothermic for both $Fe(H_2O)_n(imid)_m^{2+}$ and $Ni(H_2O)_n(imid)_m^{2+}$ complexes, and up to six water molecules can be displaced. The most favorable reaction is the displacement of the first water molecule, and for each subsequent replacement, the reactions become less favorable by approximately 2 kcal/mol because of the increased ligand−ligand repulsion. The energetics are similar for both metal ions with values slightly more favorable for Ni^{2+} because of larger electrostatic interactions for smaller ions.

Acknowledgment. A.R. was supported by NASA Contract No. NAS2-99092 to ELORET.

References and Notes

(1) Trent, J. D.; Nimmesgern, E.; Wall, J. S.; Hartl, F.-U.; Horwich, A. L. *Nature* **1991**, *354*, 490.

(2) Braig, K.; Otwinowski, Z.; Hedge, R.; Boisvert, D. C.; Joachimak, A.; Horwich, A. L.; Sigler, P. B. *Nature* **1994**, *371*, 578.

(3) Xu, Z.; Horwich, A. L.; Sigler, P. B. *Nature* **1997**, *388*, 741.

(4) Ditzel, L.; Löwe, J.; Stock, D.; Stetter, K.-O.; Huber, R.; Steinbacher, S. *Cell* **1998**, *93*, 125.

(5) Trent, J. D. Personal communication.

(6) Demoulin, D.; Pullman, A. *Theor. Chim. Acta* **1978**, *49*, 161.

(7) Garmer, D. R.; Gresh, N. *J. Am. Chem. Soc.* **1994**, *116*, 3556.

(8) Gresh, N.; Garmer, D. R. *J. Comput. Chem.* **1996**, *17*, 1481.

(9) Cini, R.; Musaev, D. G.; Marzilli, L. G.; Morokuma, K. *J. Mol. Struct. (THEOCHEM)* **1997**, *392*, 55.

(10) Peschke, M.; Blades, A. T.; Kebarle, P. *J. Am. Chem. Soc.* **2000**, *122*, 1492.

(11) Dudev, T.; Lim, C. *J. Phys. Chem. B* **2000**, *104*, 3692.

(12) Ohtaki, H.; Yamaguchi, T.; Maeda, M. *Essays on Analytical Chemistry*; Pergamon: Oxford, U.K., 1977.

(13) Marcus, Y. *Ionic Solvation*; Wiley: New York, 1985.

(14) Becke, A. D. *J. Chem. Phys.* **1993**, *98*, 5648.

(15) Stephens, P. J.; Devlin, F. J.; Chabalowski, C. F.; Frisch, M. J. *J. Phys. Chem.* **1994**, *98*, 11623.

(16) Frisch, M. J.; Pople, J. A.; Binkley, J. S. *J. Chem. Phys.* **1984**, *80*, 3265 and references therein.

(17) Wachters, A. J. H. *J. Chem. Phys*. **1970**, *52*, 1033.

(18) Hay, P. J. *J. Chem. Phys*. **1977**, *66*, 4377.

(19) Raghavachari, K.; Trucks, G. W. *J. Chem. Phys*. **1989**, *91*, 1062.

(20) Frisch, M. J.; Trucks, G. W.; Schlegel, H. B.; Scuseria, G. E.; Robb, M. A.; Cheeseman, J. R.; Zakrzewski, V. G.; Montgomery, J. A., Jr.; Stratmann, R. E.; Burant, J. C.; Dapprich, S.; Millam, J. M.; Daniels, A. D.; Kudin, K. N.; Strain, M. C.; Farkas, O.; Tomasi, J.; Barone, V.; Cossi, M.; Cammi, R.; Mennucci, B.; Pomelli, C.; Adamo, C.; Clifford, S.; Ochterski, J.; Petersson, G. A.; Ayala, P. Y.; Cui, Q.; Morokuma, K.; Malick, D. K.; Rabuck, A. D.; Raghavachari, K.; Foresman, J. B.; Cioslowski, J.; Ortiz, J. V.; Stefanov, B. B.; Liu, G.; Liashenko, A.; Piskorz, P.; Komaromi, I.; Gomperts, R.; Martin, R. L.; Fox, D. J.; Keith, T.; Al-Laham, M. A.; Peng, C. Y.; Nanayakkara, A.; Gonzalez, C.; Challacombe, M.; Gill, P. M. W.; Johnson, B. G.; Chen, W.; Wong, M. W.; Andres, J. L.; Head-Gordon, M.; Replogle, E. S.; Pople, J. A. *Gaussian 98*, revision A.9; Gaussian, Inc.: Pittsburgh, PA, 1998.

(21) Bagus, P. S.; Hermann, K.; Bauschlicher, C. W. *J. Chem. Phys*. **1984**, *80*, 4378.

(22) Bauschlicher, C. W. *Theor. Chim. Acta* **1995**, *92*, 183.

(23) Dunning, T. H. *J. Chem. Phys*. **1989**, *90*, 1007.

(24) MOLECULE-SWEDEN is an electronic structure program written by J. Almlöf, C. W. Bauschlicher, M. R. A. Blomberg, D. P. Chong, A. Heiberg, S. R. Langhoff, P.-Å. Malmqvist, A. P. Rendell, B. O. Roos, P. E. M. Siegbahn, and P. R. Taylor.

(25) Santoro, A.; Mighell, A. D.; Zocchi, M.; Reimann, C. W. *Acta Crystallogr*. **1969**, *B25*, 842.

(26) van Straten, A. J.; Smit, W. M. A. *J. Mol. Spectrosc.* **1975**, *56*, 484.

(27) Christen, D.; Griffiths, J. H.; Sheridan, J. *Z. Naturforsch.* **1981**, *36a*, 1378.